A novel surfactant protein C mutation resulting in aberrant protein processing and altered subcellular localization causes infantile interstitial lung disease

Da Hong[1], Yuanyuan Qi[1], Jing Liu[1], Huijun Wang[2], Libo Wang[1] and Liling Qian[1]

BACKGROUND: Mutations in the surfactant protein C gene (*SFTPC*) result in interstitial lung disease (ILD). Our objective was to report a novel *SFTPC* mutation and evaluate the effect of this mutant on protein synthesis and processing.

METHODS: Genomic DNA was extracted from whole blood of a Chinese infant with ILD and candidate genes associated with ILD were sequenced by next-generation sequencing. Subclones of wild-type and mutant *SFTPC* were transiently transfected into A549 cells. The functional characterization of mutant surfactant protein C (SP-C) was evaluated by Western blotting, transmission electron microscopy, and immunofluorescence.

RESULTS: A novel heterozygous mutation SFTPC: c.337T>T/C, p.Y113H was identified in this ILD infant. Neither of the parents carries this mutation. Using A549 cells expressing wild-type and mutant SP-C isoforms, Western blotting revealed a significant reduction of proSP-C and a band with abnormal molecular weight in the mutant SP-C compared to the wild-type. Ultrastructural analysis showed abnormal cytoplasmic organelles. Immunofluorescence demonstrated mutant SP-C was scarcely trafficked to lamellar bodies but localized well to early endosomes, which was in marked contrast to the wild type protein.

CONCLUSION: We detected a novel mutation in *SFTPC* causing ILD in infancy. The mutation results in aberrant proSP-C processing and altered subcellular localization.

Pulmonary surfactant is a complex mixture of lipids and proteins that is secreted to the alveolar surface by alveolar type II epithelial cells (ACE2). It reduces surface tension and prevents atelectasis at the end of expiration (1). Surfactant protein C (SP-C) is a hydrophobic, 35-amino-acid polypeptide encoded by a single gene SFTPC located on chromosome 8 (8p21). SP-C is first synthesized as a larger 21-kD precursor protein (proSP-C) and then proteolytically processed to the 3.7-kD mature form and packaged in the lamellar body, where it is stored and secreted into the airspace with surfactant protein B (SP-B) and phospholipids. Together with SP-B, SP-C enhances surfactant spreading and stability to maintain surface tension-reducing properties and gas exchange in the alveoles of the lung (2).

Interstitial lung disease (ILD) in infants and children represents a heterogeneous group of respiratory disorders that are mostly chronic and associated with high morbidity and mortality (3). In children, ILD is most frequently diagnosed in the first year of life with a predominance of genetic entities and significant advances have been made in the past decade in understanding the underlying causes for children ILD such as genetic disorders of surfactant dysfunction (4). Since Nogee *et al*. first reported a case caused by an *SFTPC* mutation in 2001 (5), more than 60 mutations in *SFTPC* have been identified in pediatric ILD patients to date. The majority of reported mutations are located in the BRICHOS domain. Several functional studies of BRICHOS mutations in *SFTPC* showed intracellular accumulation of misfolded proSP-C, which may trigger several distinct pathological mechanisms, such as induction of endoplasmic reticulum (ER) stress, cytotoxicity, and apoptosis (6–9). However, though distinct mutations within this domain are believed to lead to similar consequences, different pathomechanisms of BRICHOS mutations in *SFTPC* were implied (10,11), thus emphasizing the importance of studying single mutations in detail in order to provide a solid basis for definite diagnosis of such patients with the same mutation and develop specific therapies that target individual mutations or groups of mutations that share certain pathological features.

In the present study, we discovered a novel *SFTPC* mutation within BRICHOS domain in a Chinese ILD infant. Furthermore, mutant and wild-type *SFTPC* expression plasmids were constructed and transfected into A549 cells to investigate the functional characteristics of the novel mutation.

METHODS

Genetic Analysis

This study was approved by the ethics committees of Children's Hospital of Fudan University. Written informed consent was obtained from the patient's guardian.

The first two authors contributed equally to this work.
[1]Department of Respiratory Medicine, Children's Hospital of Fudan University, Shanghai, China; [2]The Molecular Genetic Diagnosis Center, Shanghai Key Lab of Birth Defects, Institute for Pediatric Research, Children's Hospital of Fudan University, Shanghai, China. Correspondence: Liling Qian (llqian@126.com)

Received 21 July 2016; accepted 28 December 2016; advance online publication 3 May 2017. doi:10.1038/pr.2017.29

Genomic DNA was extracted from whole blood of the patient and her parents using the QIAamp DNA Blood Mini kit (Qiagen, Hilden, Germany). DNA concentration was measured using a Nano-Drop spectrophotometer (Thermo Fisher Scientific, Waltham, MA).

Analysis of the protein-coding regions of the human *SFTPB*, *SFTPC*, *ABCA3*, *NKX2-1*, *CSF2RA*, and *CSF2RB* were performed through a self-designed gene panel using Ion Torrent PGM (Life Technologies, Carlsbad, CA). Targeted genomic regions covered exons from the major isoform of the six genes responsible for surfactant dysfunction. Exon coordinates were extended to an additional 50 bp in flanking intronic sequences. Primer design for multiplex amplification was performed with Ion AmpliSeq Designer version 2.2 (Life Technologies). Library preparation for next-generation sequencing of the targeted genes was performed by multiplex amplification using the Ion AmpliSeq Library Kit 2.0 (Life Technologies). Patient sample was then barcoded using Ion Xpress Barcode Kit (Life Technologies). The amplified librairy was purified using Agencourt AMPure XP Beads (Beckman Coulter, Brea, CA). The concentration of the library was determined using Ion Library TaqMan quantitation assay kit (Thermo Fisher Scientific, Waltham, MA). We used the Ion OneTouch system (Life Technologies) to clonally amplify pooled barcoded libraries on Ion Sphere particles (Life Technologies). Sequencing was undertaken using 316 v2 chips (Life Technologies) on the Ion Torrent PGM. Torrent Suite software (Life Technologies) was used to compare base calls. NextGENe software (SoftGenetics, State College, PA) was used to read alignments and to call variant with the human genomic reference hg19 (NCBI, Bethesda, MD). The variants selected for further analysis met the following criteria: (i) The variant was detected in sequence reads for both strands, (ii) a minimum coverage of 20× was achieved, (iii) the variant reads represented >20% of the sequence reads at a particular site, (iv) the targeted region covered all exons and at least 20 bp of all intron/splice sites. The filtered variants were then compared with dbSNP (http://www.ncbi.nlm.nih.gov/projects/SNP/). Novel variants of unknown significance (VUS) were analyzed with in silico tools MutationTaster (http://www.mutationtaster.org/), SIFT (http://sift.jcvi.org/) and PolyPhen2 (http://genetics.bwh.harvard.edu/pph2/).

The variant was validated by PCR followed by direct Sanger sequencing using 3500XL Genetic Analyzer (Applied Biosystems, Foster City, CA).

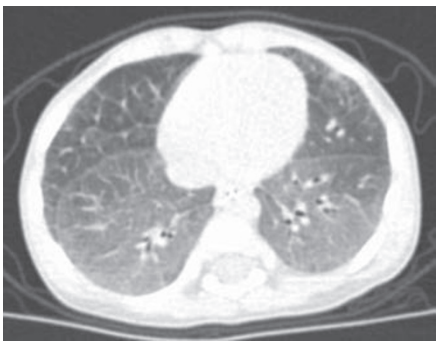

Figure 1. Chest high resolution CT scan at 5 months of age. High-resolution computed tomography showed bilateral reticular and ground-glass changes with small subpleural cyst.

SFTPC cDNA Expression Constructs

A full-length human *SFTPC* cDNA clone (NM_003018) was purchased from Youbio (Changsha, China). Using it as a template, the Flag tag (DYKDDDDK) was added to both the N-terminus and C-terminus of SP-C. The 5′ (forward) primer contained an EcoR1 enzyme site (bold) and the Flag coding sequence (underlined): CCG**GAATTC**ATGGACTACAAGGACGACGATGACAAGATGG ATGTGGGCAGCAAAGA. The 3′ (reverse) primer contained a BamH1 site (bold) and the Flag coding sequence (underlined): CGC **GGATCC**CTACTTGTCATCGTCGTCCTTGTAGTCGATGTAGT AGAGCGGCATTC. Following amplification, the purified fusion insert was subcloned into the pCDH-EGFP expression vector which was from our own lab using digestion with EcoR1 and BamH1.

For construction of mutant Flag/SP-C^{Y113H}, mutagenesis was performed by inverse PCR using KOD Plus Mutagenesis Kit (Toyobo, Osaka, Japan) with pCDH-EGFP-Flag/SP-C^{WT} serving as a template. The 5′ (forward) primer used for mutagenesis: CACA AGCCAGCCCCTGGCACCTGCTGC. The 3′ (reverse) primer: GGCGATCAGCAGCTGCTGGTAGTCATA. Both constructs were confirmed by direct Sanger sequencing.

A549 Cell Line and Transfection

Human A549 lung epithelial cells were kindly provided by Stem Cell Bank, Chinese Academy of Sciences. A549 cells grown to 70% confluence were transiently transfected with Flag/SP-C^{WT} or Flag/SP-C^{Y113H} using Lipofectamine 3000 Transfection Reagent (Thermo Fisher Scientific) according to the manufacturer's instructions. The medium was replaced at 24 h, and transfected cells were maintained for up to 48 h.

Western Blotting

Transfected A549 cells were cultured for 48 h, harvested and subjected to protein extraction. Thirty micrograms of total protein was separated in 10% SDS polyacrylamide gels, then transferred to nitrocellulose membrane. Mouse anti-Flag (1:3,000; Abmart, Shanghai, China), rabbit anti-Pro-SP-C (1:5,000; Seven Hills Bioreagents, Cincinnati, OH), rabbit anti-XBP1 (1:500; Abcam, Cambridge, UK), rabbit anti-GRP78 (1:700; Abcam) and mouse anti-β-tubulin (1:3,000; CST, Danvers, MA) were used as primary antibodies. Goat anti-mouse and Goat anti-rabbit horseradish peroxidase-conjugated antibody (Abcam) was used as secondary antibody. β-tubulin was used as the standard for normalizing protein samples. Bands were visualized by enhanced chemiluminescence.

Transmission Electron Microscopy

Transfected A549 cells were cultured for 48 h and fixed. After dehydration through a series of ethanol gradients, the samples were embedded in EPON resin. Ultrathin sections (70 nm) were prepared and

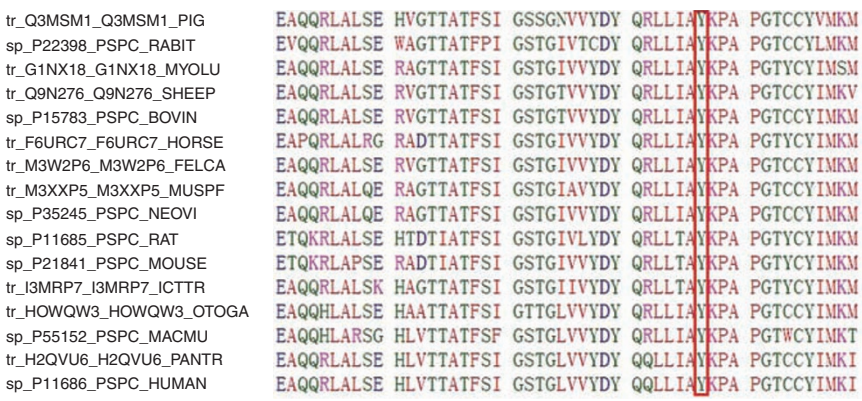

Figure 2. Partial amino acid alignment of SP-C sequence. Alignment shows the Tyr113 (indicated by red box) was highly conserved.

double-stained with uranyl acetate and lead citrate. Ultrastructural analysis was carried out using transmission electron microscope (JEM-1400; Jeol, Tokyo, Japan).

Immunofluorescence

Forty-eight hours after transfection, cells grown on glass bottom cell culture dishes were fixed with 4% paraformaldehyde, permeabilized with 0.2% Triton X-100, and blocked for 1 h in 3% FBS. The following primary antibodies were used: mouse anti-Flag (1:1,000; Abmart, Shanghai, China), rabbit anti-CD63 (1:100; Santa Cruz, Dallas, TX), rabbit anti-EEA1 (1:500; Abcam), rabbit anti-calnexin (1:200; Abcam) and rabbit anti-ubiquitin (1:100; Abcam). Species specific Alexa Fluor 647 and Alexa Fluor 555 secondary antibodies (Invitrogen, Waltham, MA) were used at 1:200. Samples were mounted and Alexa Fluor fluorescence was examined using Leica TCS SP8 confocal laser scanning microscope (Leica, Jena, Germany).

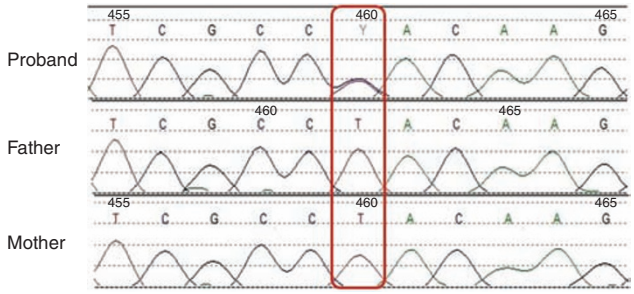

Figure 3. The heterozygous p.Y113H mutation was validated by Sanger sequencing. Both parents are negative for this mutation suggesting it arise *de novo*.

RESULTS

Case Summary

The patient was a full-term (40 wk) female born to nonconsanguineous healthy parents. The pregnancy and delivery were uneventful with a birth weight of 3,300 g. The infant was asymptomatic until 7 d of life when she presented with cough and patchy infiltrates in the right lung on chest x-ray. She was admitted to our hospital at 13 d of life with a diagnosis of neonatal pneumonia and patent foramen ovale (1.9 mm), treated with antibiotics and supplemental oxygen for 17 d and discharged home with significant improvement. However, the infant continued to have cough, tachypnea and exhibited failure to thrive after discharge. She was admitted again at 2 mo of age due to aggravating symptoms. Screening for infectious and immunologic etiologies was negative. Chest x-ray showed patchy infiltrates in both lungs. The patient was treated with antibiotics and nasal oxygen for 15 d without

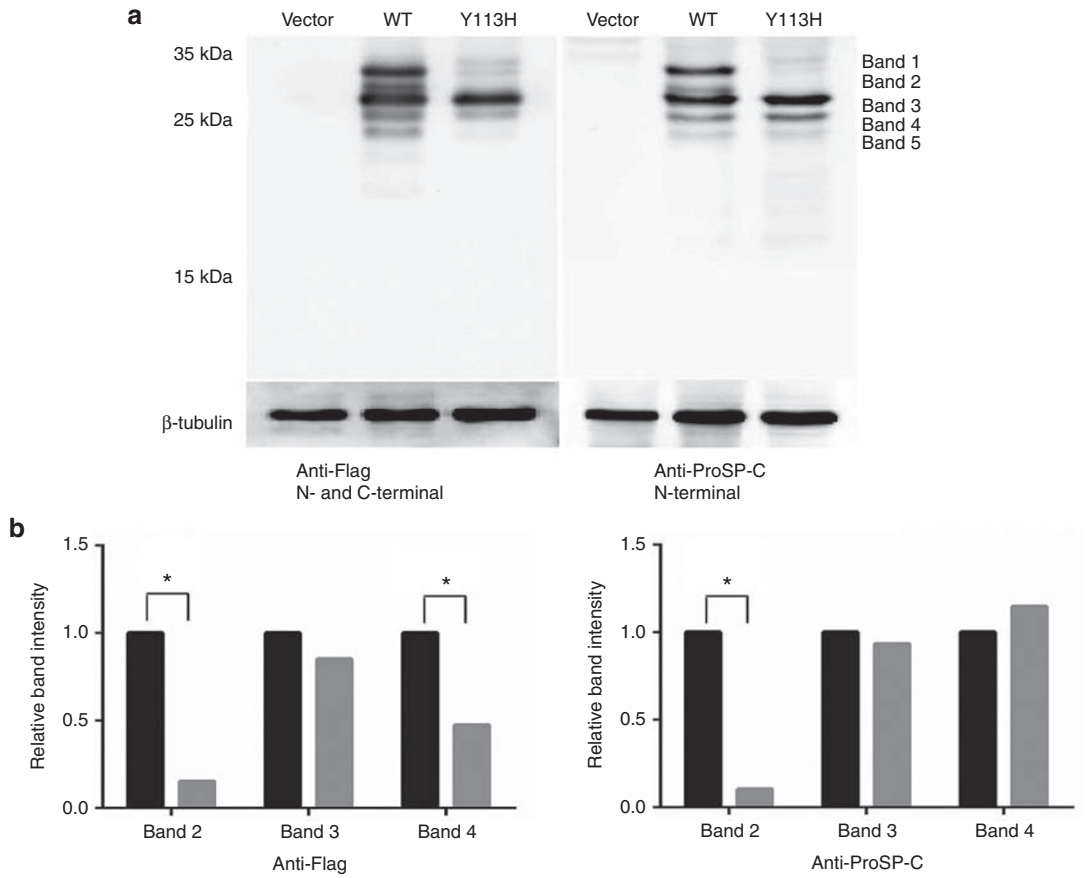

Figure 4. Processing features of proSP-C^{WT} and proSP-C^{Y113H}. (**a**) Western blotting of total protein from A549 cells transfected with pCDH-EGFP vector, Flag/SP-C^{WT} or Flag/SP-C^{Y113H} using antibodies against flag tag (left) and proSP-C (right) respectively was performed. An aberrant band and several reduced processing intermediates in SP-C^{Y113H} were observed as compared to the wild type. (**b**) Band intensity of band 2, 3 and 4 which could be detected in both the wild-type and mutant was quantified and results from at least three separate experiments are shown. Data of mutant SP-C (gray column) were expressed as fold change over the wild-type (black column) values in each experiment. β-tubulin bands were used to normalize for equal loading. $^{*}P < 0.05$, $^{**}P < 0.001$.

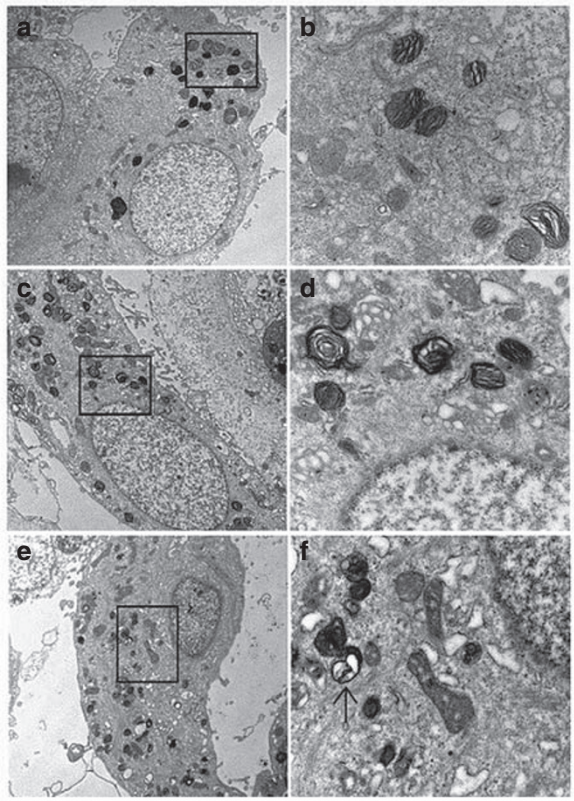

Figure 5. Ultrastructural features of A549 cells transfected with proSP-C^{WT} and proSP-C^{Y113H} by transmission electron microscopy. Solid boxes on the left (scale bars = 2 μm) were magnified for better resolution (right) (scale bars = 500 nm). (**a, b**): In nontransfected A549 cells, various cellular components such as endosomes and lysosomes were observed. (**c, d**) In cells transfected with proSP-C^{WT}, a markedly increased number of organelles were noted including multiple concentrically packed organelles resembling lamellar bodies. (**e, f**) In A549 cells transfected with proSP-C^{Y113H}, Numerous disorganized lysosomal-like organelles with hollow or eccentrically packed inclusions (arrow) were observed.

obvious improvement in symptoms and chest radiograph. Considering the persistent yet clinically stable condition, she was discharged with home oxygen therapy and close follow-up. During the outpatient follow-up, although respiratory symptoms of the patient improved slightly, failure to thrive persisted. High-resolution computed tomography at 5 mo of age showed bilateral reticular and ground-glass changes with small subpleural cyst (**Figure 1**). Now the patient is 10-mo old still on home oxygen therapy with lower flow and under regular outpatient follow-up.

Genetic Analysis

Next-generation sequencing of candidate genes responsible for surfactant dysfunction (including *SFTPB*, *SFTPC*, *ABCA3*, *NKX2-1*, *CSF2RA*, and *CSF2RB*), which was performed at 3 mo of age in the patient revealed a heterozygous missense mutation c.337T>T/C at codon 113 in exon 4 of *SFTPC* which results in a substitution of tyrosine for histidine (*SFTPC*: c.337T>T/C, p. Y113H). This mutation is located in the BRICHOS domain and the amino acid residue is highly conserved across mammal species (**Figure 2**). The variant is not found in publically available human exome databases such as dbSNP, ExAC (http://exac.broadinstitute.org/) and 1000 genomes (http://www.1000genomes.org/) indicating it is an extremely rare mutation. It is predicted to be disease-causing or damaging by MutationTaster, SIFT and PolyPhen2. Neither of the parents carries this mutation suggesting it is a *de novo* mutation (**Figure 3**). Both parents were healthy without a history of previous lung disease except that the father had pulmonary tuberculosis several years ago which had already been cured.

In Vitro Analysis of SP-C Expression

To identify potential processing differences between proSP-C^{WT} and proSP-C^{Y113H}, lysates of A549 cells transiently transfected with Flag/SP-C^{WT} or Flag/SP-C^{Y113H} expression constructs were analyzed by Western blotting using anti-Flag antibody or anti-Pro-SP-C antibody respectively. As is shown in **Figure 4** (left), when using anti-flag antibody recognizing flag tag at both terminals of the fusion protein, two strong bands at ~31 kDa (band 2) and 26 kDa (band 3) as well as three weak bands between 20-30kDa were visualized for proSP-C^{WT}. In comparison, a different pattern was observed for proSP-C^{Y113H}. We observed a band at 32 kDa (band 1) that was not seen in the wild type. Meanwhile, a band at 27 kDa detectable in proSP-C^{WT} was missing in proSP-C^{Y113H}. In addition, bands 2 and 5 were significantly reduced as compared to those in proSP-C^{WT}. Similar results were observed for anti-Pro-SP-C antibody binding to the N-terminus of proSP-C (**Figure 4**, right), except for that band 5 of the wild-type and mutant proteins seemed to be at equal level.

Aberrant Ultrastructure of ProSP-C^{Y113H}-Transfected A549 Cells

To characterize the structure of subcellular organelles in A549 cells transfected with proSP-C^{WT} and proSP-C^{Y113H}, ultrastructural analysis by transmission electron microscopy was performed. In the nontransfected A549 cells, various cellular components such as endosomes and lysosomes were present within the cytoplasm (**Figure 5a**,**b**). A markedly increased number of organelles were noted in transfected A549 cells suggesting an overexpression of transfected *SFTPC* genes. Multiple concentrically packed organelles resembling lamellar bodies were evident in cells transfected with proSP-C^{WT} (**Figure 5c**,**d**). Numerous disorganized lysosomal-like organelles with hollow or eccentrically packed inclusions were observed in A549 cells transfected with proSP-C^{Y113H} (**Figure 5e**,**f**).

Abnormal Subcellular Localization of ProSP-C^{Y113H}

Immunofluorescence analysis showed that the intracellular localization of proproteins differed between A549 cells expressing proSP-C^{WT} and proSP-C^{Y113H}. ProSP-C^{WT} was localized to CD63 (a marker for lamellar bodies and lysosomes)-positive and EEA1 (an early endosome marker)-negative vesicles, the expected target vesicle for the wild-type isoform of SP-C. In contrast, proSP-C^{Y113H} scarcely colocalized with CD63 but localized well with EEA1 suggesting abnormal trafficking and accumulation in early endosomes (**Figure 6a**,**b**). To assess the

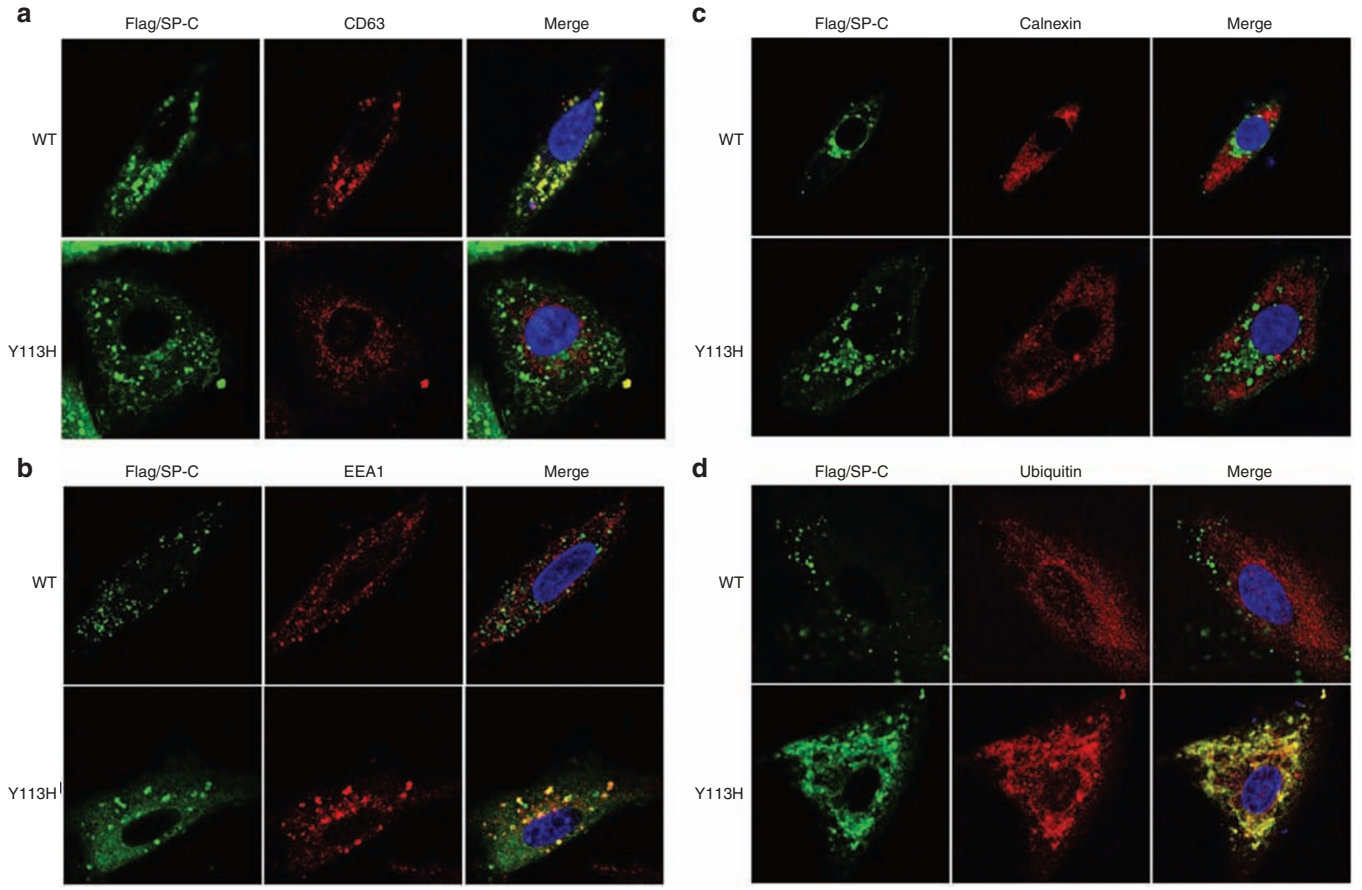

Figure 6. Intracellular localization of proSP-C^{WT} and proSP-C^{Y113H} forms in transfected A549 cells. Green channel: proSP-C visualized by anti-Flag antibody; Merge: green and red channel merged to visualize colocalization (yellow). Nuclei were visualized by DAPI (4′6-diamidino-2-phenylindole, blue). Red channel: (**a**) CD63, a marker for lamellar bodies and lysosomes. ProSP-C^{WT} localized to CD63 while proSP-C^{Y113H} did not. (**b**) EEA1, a marker for early endosome. ProSP-C^{Y113H} localized to EEA1 which was not observed for proSP-C^{WT}. (**c**) Calnexin, a common marker for endoplasmic reticulum (ER). Neither of proSP-C^{WT} and proSP-C^{Y113H} localized to calnexin. (**d**) Ubiquitin. Complete colocalization with ubiquitin was visualized for proSP-C^{Y113H} which was not seen in proSP-C^{WT}.

fate of mutant SP-C, immunofluorescence analysis of ubiquitin was also performed. While proSP-C^{WT} hardly colocalized with ubiquitin, almost complete colocalization was observed for proSP-C^{Y113H} (**Figure 6d**).

Previous studies showed that some *SFTPC* mutations lead to an increase in ER stress (12). However, no colocalization with the ER marker calnexin was observed for both proSP-C^{WT} and proSP-C^{Y113H} indicating no ER retention induced by this Y113H mutation (**Figure 6c**). To further ascertain the presence or absence of ER stress, expression of two well-recognized unfolded protein response (UPR) genes, XBP1 and GRP78, was assessed by Western blotting. As seen in **Figure 7**, no difference in expression of XBP-1 and GRP78 was observed between proSP-C^{WT} and proSP-C^{Y113H} transfected cells. Tunicamycin (TM), an ER stress inducer used as a positive control, considerably increased the expression of both UPR gene products.

DISCUSSION

In this study, we described a Chinese ILD infant whose clinical course and radiological findings were consistent with previous reports of surfactant dysfunction (13–15). High-throughput sequencing revealed a novel heterozygous mutation in BRICHOS domain of *SFTPC* (*SFTPC*: c.337T>T/C, p. Y113H). This variant is not found in dbSNP, ExAC, 1000 genomes and predicted to be damaging by MutationTaster, SIFT and PolyPhen2. Furthermore, neither of the parents carries this mutation suggesting it arose de novo. All these evidence supports the pathogenic nature of this missense mutation.

To investigate the functional impact of the Y113H mutation, *in vitro* expression of mutant SP-C was analyzed in transfected A549 cells. According to previous research, most of *SFTPC* mutations in the BRICHOS domain, such as A116D, exon 4 deletion and L188Q, were associated with chronic accumulation of misfolded proSP-C while mutations located in the non-BRICHOS region like I73T and L55F misdirected proSP-C to the plasma membrane, leading to the accumulation of abnormally processed isoforms (8,10,16–18). However, in our Western blotting analysis, no accumulated proprotein was observed for proSP-C^{Y113H}. Instead, a significant reduction in different isoforms especially those lower than 25 kDa was evident as compared to proSP-C^{WT}, which indicated an arrest of protein processing at certain stage or excessive degradation of misfolded proSP-C^{Y113H}. Although band 3 which

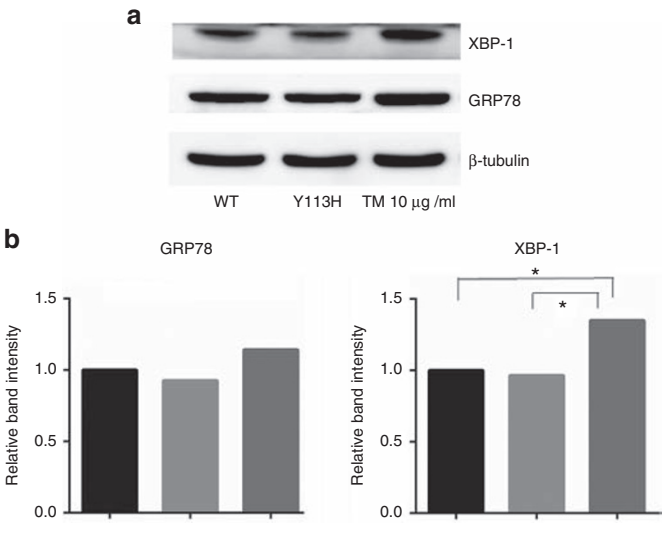

Figure 7. Unfolded protein response (UPR) gene expression in A549 cells transfected with proSP-C^{WT} and proSP-C^{Y113H}. (**a**) Representative immunoblot bands of two well-recognized UPR gene products, XBP-1 and GRP78. For both proteins, no difference was observed between proSP-C^{WT} and proSP-C^{Y113H} transfected cells. Tunicamycin (TM)-treated A549 cells were used as a positive control. (**b**) Quantitation of band intensity normalized to β-tubulin from three separate experiments. Data of the mutant (gray column) and TM-treated (dark gray column) cells were expressed as fold change over the wild-type (black column) values in each experiment. β-tubulin bands were used to normalize for equal loading. *$P < 0.05$.

likely corresponded to the primary translation product of the fusion protein showed no difference, an aberrant 32 kDa band as well as a reduced 31 kDa band which may correspond to palmitoylated isoforms of the primary translation product of the fusion protein was identified for proSP-C^{Y113H} suggesting a probability of abnormal post-translational modification.

Immunofluorescence assay of transfected A549 cells showed proSP-C^{Y113H} predominantly colocalized with EEA1 but not with lamellar body marker CD63, which is similar to previous studies on *SFTPC* mutations such as A116D and I73T (6,19). Meanwhile, complete colocalization with ubiquitin was noted for proSP-C^{Y113H}, suggesting the mutant SP-C entered ubiquitin-mediated degradation. The level of individual plasma membrane proteins such as SP-C needs to be regulated strictly depending on the situation under which the cell is placed. To reduce the level of a specific plasma membrane protein in a short period, cells internalize the protein from the cell surface by endocytosis and degrade it through the endocytic pathway involving early endosome and lysosome (20,21). Ubiquitin acts as a sorting signal in the endomembrane system to target the mutant proteins into the vacuolar degradation pathway (22). All our data, together with ultrastructural images, highly suggest that physiological proSP-C^{WT} forms are secreted via lamellar body fusion with the plasma membrane and then catabolized mainly by alveolar macrophages. However, abnormally modified or processed proSPC^{Y113H} forms might be secreted by a different route, accumulated in the alveolar lumen which is supported by alveolar proteinosis observed in patients, and eventually stimulate endocytosis of ACE2 to recycle or degrade these mutant protein.

It has previously been shown that SP-C mutations lead to ER stress. The ER has developed a tightly regulated quality control mechanism such that even the slightest alteration in a protein's makeup that disturbs folding efficacy can cause the recognition of the nascent protein as misfolded, leading to subsequent accumulation and/or retrotranslocation of the protein to the cytosol. In the cytosol, misfolded proteins are primarily destined for proteasome-mediated ER-associated degradation (7). However, in our study, no colocalization with ER marker calnexin was observed for proSP-C^{Y113H}.

Genetic disorders of surfactant dysfunction are known rare causes of pediatric lung diseases including neonatal respiratory distress syndrome (NRDS) and children's ILD. Mutations in genes encoding proteins important in surfactant production and function (SP-B, SP-C, and ABCA3), surfactant catabolism (GM-CSF receptor), as well as transcription factors important for surfactant production (NKX2-1) disrupt surfactant homeostasis and result in acute or chronic lung disease (4,23). Because of the overlapping phenotypes of different disease-causing genes, a priority strategy for genetic diagnosis was recommended from Nogee LM with a combination of clinical and pathological presentation (4). However, thanks to the rapid advance in sequencing technology, next-generation sequencing covering all these genes provides a more efficient and non-invasive approach to interrogate the genetic basis of patients with suspected surfactant dysfunction.

A limitation of the study is that parents declined lung biopsy so that no lung sample of the infant is available. Therefore *in vivo* data regarding mutant SP-C expression remain unclear. Moreover, our *in vitro* system corresponds rather to a homozygous than to a heterozygous *SFTPC* mutation where one wild type copy is still present. Additional *in vivo* models are needed to further elucidate detailed mechanism of the *SFTPC* Y113H mutation.

In summary, we reported a novel disease-causing mutation in BRICHOS domain of *SFTPC* in a Chinese ILD infant. Functional study of A549 cells transfected with mutant Y133H *SFTPC* gene indicated that the mutation may result in aberrant proSP-C processing and altered subcellular localization.

STATEMENT OF FINANCIAL SUPPORT

This study was supported by grants from the Shanghai Committee of Science and Technology (No. 134119a7800 and No.14411962102), the Development Fund for Shanghai talents (201450).

Disclosure: We have no financial disclosures indicating any financial ties to products in the study or potential/perceived conflicts of interest.

REFERENCES

1. Serrano AG, Pérez-Gil J. Protein-lipid interactions and surface activity in the pulmonary surfactant system. Chem Phys Lipids 2006;141:105–18.
2. Whitsett JA, Weaver TE. Hydrophobic surfactant proteins in lung function and disease. N Engl J Med 2002;347:2141–8.
3. Clement A, Eber E. Interstitial lung diseases in infants and children. Eur Respir J 2008;31:658–66.
4. Nogee LM. Genetic basis of children's interstitial lung disease. Pediatr Allergy Immunol Pulmonol 2010;23:15–24.
5. Maitra M, Cano CA, Garcia CK. Mutant surfactant A2 proteins associated with familial pulmonary fibrosis and lung cancer induce TGF-β1 secretion. Proc Natl Acad Sci USA 2012;109:21064–9.

6. Zarbock R, Woischnik M, Sparr C, et al. The surfactant protein C mutation A116D alters cellular processing, stress tolerance, surfactant lipid composition, and immune cell activation. BMC Pulm Med 2012;12:15.
7. Mulugeta S, Maguire JA, Newitt JL, Russo SJ, Kotorashvili A, Beers MF. Misfolded BRICHOS SP-C mutant proteins induce apoptosis via caspase-4- and cytochrome c-related mechanisms. Am J Physiol Lung Cell Mol Physiol 2007;293:L720–9.
8. Mulugeta S, Nguyen V, Russo SJ, Muniswamy M, Beers MF. A surfactant protein C precursor protein BRICHOS domain mutation causes endoplasmic reticulum stress, proteasome dysfunction, and caspase 3 activation. Am J Respir Cell Mol Biol 2005;32:521–30.
9. Lawson WE, Crossno PF, Polosukhin VV, et al. Endoplasmic reticulum stress in alveolar epithelial cells is prominent in IPF: association with altered surfactant protein processing and herpesvirus infection. Am J Physiol Lung Cell Mol Physiol 2008;294:L1119–26.
10. Thurm T, Kaltenborn E, Kern S, Griese M, Zarbock R. SFTPC mutations cause SP-C degradation and aggregate formation without increasing ER stress. Eur J Clin Invest 2013;43:791–800.
11. Stewart GA, Ridsdale R, Martin EP, et al. 4-Phenylbutyric acid treatment rescues trafficking and processing of a mutant surfactant protein-C. Am J Respir Cell Mol Biol 2012;47:324–31.
12. Maguire JA, Mulugeta S, Beers MF. Endoplasmic reticulum stress induced by surfactant protein C BRICHOS mutants promotes proinflammatory signaling by epithelial cells. Am J Respir Cell Mol Biol 2011;44:404–14.
13. Guillot L, Epaud R, Thouvenin G, et al. New surfactant protein C gene mutations associated with diffuse lung disease. J Med Genet 2009;46:490–4.
14. Avital A, Hevroni A, Godfrey S, et al. Natural history of five children with surfactant protein C mutations and interstitial lung disease. Pediatr Pulmonol 2014;49:1097–105.
15. Kröner C, Reu S, Teusch V, et al. Genotype alone does not predict the clinical course of SFTPC deficiency in paediatric patients. Eur Respir J 2015;46:197–206.
16. Liu T, Sano K, Ogiwara N, Kobayashi N. A novel surfactant protein C L55F mutation associated with interstitial lung disease alters subcellular localization of proSP-C in A549 cells. Pediatr Res 2016;79:27–33.
17. Wang WJ, Mulugeta S, Russo SJ, Beers MF. Deletion of exon 4 from human surfactant protein C results in aggresome formation and generation of a dominant negative. J Cell Sci 2003;116(Pt 4):683–92.
18. Hawkins A, Guttentag SH, Deterding R, et al. A non-BRICHOS SFTPC mutant (SP-CI73T) linked to interstitial lung disease promotes a late block in macroautophagy disrupting cellular proteostasis and mitophagy. Am J Physiol Lung Cell Mol Physiol 2015;308:L33–47.
19. Woischnik M, Sparr C, Kern S, et al. A non-BRICHOS surfactant protein c mutation disrupts epithelial cell function and intercellular signaling. BMC Cell Biol 2010;11:88.
20. Spang A. On the fate of early endosomes. Biol Chem 2009;390:753–9.
21. Tanno H, Komada M. The ubiquitin code and its decoding machinery in the endocytic pathway. J Biochem 2013;153:497–504.
22. Scheuring D, Künzl F, Viotti C, et al. Ubiquitin initiates sorting of Golgi and plasma membrane proteins into the vacuolar degradation pathway. BMC Plant Biol 2012;12:164.
23. Whitsett JA, Wert SE, Weaver TE. Alveolar surfactant homeostasis and the pathogenesis of pulmonary disease. Annu Rev Med 2010;61:105–19.